Special Issue Article

Journal of Molecular Recognition

Received: 13 January 2012, Revised: 20 August 2012, Accepted: 21 August 2012, Published online in Wiley Online Library

(wileyonlinelibrary.com) DOI: 10.1002/jmr.2223

Elution relationships to model affinity chromatography using a general rate model†

Gabriela Sandoval, Barbara A. Andrews and Juan A. Asenjo*

Different mathematical models with different degrees of complexity have been proposed to model affinity chromatography. In this work, in particular, a general rate model has been studied that considers axial dispersion, external film mass transfer, intraparticle diffusion, and kinetic effects investigating the influence in the simulations of two different relationships between the properties of the mobile phase and the affinity of different proteins to the ligand bound to the matrix. Two systems were used: Blue Sepharose and Protein A. With Blue Sepharose, an increasing linear salt gradient was used, and with Protein A, a decreasing semi-linear pH gradient. The kinetic parameters obtained in each of the two elution (adsorption/desorption) relationships studied (a power law type and an exponential type) led to very good agreements between experimental and simulated elution curves of mixtures of proteins finding that for more symmetrical peaks, the preferred elution relationship should be the exponential one, in contrast to the more asymmetrical peaks which shapes are better simulated by the power law relationship. Copyright © 2012 John Wiley & Sons, Ltd.

Keywords: affinity chromatography; rate model; elution (adsorption/desorption) relationships

INTRODUCTION

Several papers can be found in the literature that present models to simulate protein elution curves of different types of chromatography (Yamamoto *et al*., 1983; Gallant *et al*., 1996; Li *et al*., 1998; Gu and Zheng, 1999; Gu *et al*., 2003; Shene *et al*., 2006; Lienqueo *et al*., 2009; Orellana *et al*., 2009). In particular, for affinity chromatography, there is work from Gu and coworkers (2003) who use a general rate model with a second-order kinetic binding reaction including size exclusion factors. Li and coworkers (2004) also use a general rate model but using the steric mass action formulism to model the binary adsorption isotherm. Their results were compared with those obtained by our group (Sandoval *et al*., 2010) where we proposed an exponential type of elution (adsorption/desorption) relationship different from that described by Gu and coworkers (1992). In this paper, we compare the results of simulating two different systems of affinity chromatography using an exponential type elution relationship and a power law relationship such as the one presented by Melander and coworkers (1989) and studied by Gu and coworkers (1992) to model isocratic, linear, and nonlinear gradient elution chromatography.

Mathematical modeling

General rate model

The model studied in this work, presented by Gu (1995) and formulated for affinity chromatography in Sandoval *et al*. (2010), consists of a set of two partial differential equations that accounts for the mass transfer of the components (proteins and modulator) in the mobile phase along the column and in the interior of the matrix particles. These sets of equations are coupled together by a set of ordinary differential equations that describe the adsorption kinetics of the components to the matrix. In the dimensionless form, the equations studied are as follows. First, the mass balance for the components in the bulk fluid phase is given by Eq. (1):

$$-\frac{1}{\mathrm{Pe}_{Li}}\frac{\partial^2 c_{bi}}{\partial z^2}+\frac{\partial c_{bi}}{\partial z}+\frac{\partial c_{bi}}{\partial \tau}+\xi_i\left(c_{bi}-c_{pi,r=1}\right)=0 \tag{1}$$

For the modulator (ionic strength or pH), the fourth term was not considered.

The mass balance for the components in the fluid inside the porous particles is given by Eq. (2):

$$\left(1-\varepsilon_p\right)\frac{\partial c_{pi}^*}{\partial \tau}+\varepsilon_p\frac{\partial c_{pi}}{\partial \tau}-\eta_i\left[\frac{1}{r^2}\frac{\partial}{\partial r}\left(r^2\frac{\partial c_{pi}}{\partial r}\right)\right]=0 \tag{2}$$

These sets of equations are coupled together by the second-order kinetic binding expression shown in Eq. (3):

$$\frac{\partial c_{pi}^*}{\partial \tau}=\mathrm{Da}_i^a c_{pi}\left(c_i^\infty-\sum_{j=1}^{N}\frac{C_{oj}}{C_{oi}}c_{pj}^*\right)-\mathrm{Da}_i^d c_{pi}^* \tag{3}$$

The initial and boundary conditions are given by Eqs (4) and (5).

$$\left.\begin{array}{l} c_{bi}(0,z)=0 \\ \dfrac{\partial c_{bi}(\tau,0)}{\partial z}=\mathrm{Pe}_{Li}\left[c_{bi}(\tau,0)-\dfrac{C_{fi}(\tau)}{C_{oi}}\right] \\ \dfrac{\partial c_{bi}(\tau,1)}{\partial z}=0 \end{array}\right\} i=1,\ldots,N+1 \tag{4}$$

* Correspondence to: Juan Asenjo, University of Chile, Santiago, Chile. E-mail: juasenjo@ing.uchile.cl

† This article is published in Journal of Molecular Recognition as part of the special issue on Affinity 2011 - The 19th biennial meeting of the International Society for Molecular Recognition, edited by Gideon Fleminger (Tel-Aviv University, Israel) and George Ehrlich (Hoffmann-La Roche, Nutley, NJ).

G. Sandoval, B. A. Andrews, J. A. Asenjo
University of Chile, Santiago, Chile

$$\left.\begin{array}{c} c_{pi}(0,z,r)=0, \quad c_{\overline{pi}}(0,z,r)=0 \\ \dfrac{\partial c_{pi}(\tau,0,z)}{\partial r}=0 \\ \dfrac{\partial c_{pi}(\tau,1,z)}{\partial r}=\mathrm{Bi}_i\left[c_{bi}(\tau,z)-c_{pi}(\tau,z,1)\right] \end{array}\right\} i=1,\ldots,N \quad (5)$$

Elution relationships

Gu (1995) stated that one can use any relationship between components and modulator as long as the computational results have a good agreement with the experimental data. According to this, two elution (adsorption/desorption) relationships were used in this study: a modification of the relationship proposed by Melander and coworkers (1989) and a modification of the relationship proposed by Sandoval and coworkers (2010).

Power elution relationship

This relationship is a modification of the one proposed by Melander and coworkers (1989) that preservers the physical and hydrophobic interactions between the proteins (components $i=1,\ldots,N$) inside the particle and the modulator (component $i=N+1$) in the mobile phase, as shown in Eq. (6):

$$Da_i^q = C_{0i} Da_i^d 10^{\alpha_i+\gamma_i c_{b,N+1}} \quad (6)$$

To use this relationship, one needs to determine the Damkhöler number for desorption and the parameters α_i and γ_i for each individual protein.

Exponential elution relationship

This relationship (Eq. (7)) is a modification of the one presented by Sandoval and coworkers (2010) and allows a better simulation of the elution curves of proteins in a mixture.

$$Da_i^d = \alpha_i'\left(e^{\beta'_i\left(c_{b,N+1}-c_{A,N+1}\right)}-1\right) \quad (7)$$

To use this relationship, one needs to determine the Damkhöler number for adsorption and the parameters α_i' and β_i' for each individual protein.

Mathematical simulation

The general rate model, with the respective elution relationships, was solved using Matlab® 2009. The two sets of partial differential equations (Eqs (1) and (2)) were discretized using finite elements (with 5 quadratic elements, N_B) and orthogonal collocation (with 2 and 3 internal nodes, N_r) methods as shown in Gu (1995), to obtain two sets of ordinary differential equations that were coupled by the kinetic expression shown in Eq. (3). The final system of ordinary differential equations was solved using the Matlab® *ode15s* routine.

Parameter estimation

The physical parameters used in simulations are presented in Table 1. The dimensionless parameters present in the rate model were estimated using the correlations presented in Table 2.

MATERIALS AND METHODS

Experimental procedure

The chromatograms of individual proteins and mixtures were obtained using the methodology presented in Sandoval *et al.* (2010). The operational conditions used to obtain the curves of individual proteins in order to determine the parameters of the different elution relationships studied in this work are presented in Table 3, and those used to obtain chromatograms of mixtures of proteins are shown in Tables 4 and 5.

Table 1. Physical parameters used in simulations

Parameter	Value or range of values		
	Blue Sepharose		Protein A
Column capacity, C^{∞} (mg/ml)	11[a]		50[c]
Density of the mobile phase, ρ_l (g/cm^3)	0.99823[b]		0.99823[b]
Inner diameter of the column (cm)	0.5[c]		0.7[c]
Macroporous particle diameter, d_{porous} (nm)	300[d]		700[d]
Bed void volume fraction, ε_b	0.4[e]		0.4[e]
Column length, L (cm)	5[c]		2.5[c]
Molecular weight, MW_i (kDa)	BSA	66.0[a]	150[a]
	Hb	64.5[a]	
Particle porosity, ε_p	BSA	0.55[f]	0.55
	Hb	0.58[f]	
Particle radius, R_p (cm)	0.0045		0.0045[c]
Tortuosity, τ_{tor}	(2–6)[e]		(2–6)[e]
Viscosity of the mobile phase, μ_l (g/(cm·s))	0.01005[b]		0.01005[b]

[a]Sigma-Aldrich Co. Catalog numbers: R9903 (Blue Sepharose CL-6B), A7030 (bovine serum albumin), H7255 (hemoglobin from rabbit), M5284 (mouse IgG1), M5409 (mouse IgG2a), M5534 (mouse IgG2b)
[b]Geankoplis, 1998
[c]GE Healthcare, HiTraprProtein A FF. Catalog number 17-5079-02
[d]Hage *et al.*, 2006
[e]Gu *et al.*, 2003 and Li *et al.*, 2004
[f]Li *et al.*, 2004

Table 2. Correlations used for parameter estimation

Correlation	Reference
$Pe_{Li} = \frac{L}{2R_p \varepsilon_b}(0.2 + 0.011\mathrm{Re}^{0.48})$, valid for $10^{-3} < \mathrm{Re} < \boldsymbol{10}^{3}$	Chung and Wen (1968)
$D_{pi}\left(\frac{cm^2}{s}\right) = \frac{D_{mi}}{\tau_{tor}}(1 - 2.104\lambda_i + 2.09\lambda_i^3 - 0.95\lambda_i^5)$	Yau *et al.* (1979)
$d_{mi}(\boldsymbol{A}) = 1.44 MW_i^{\frac{1}{3}}$ valid for hydrated proteins	Gu and Zheng (1999)
$D_{mi}\left(\frac{cm^2}{s}\right) = 2.74 \cdot 10^{-5} MW_i^{\frac{1}{3}}$ valid for $MW_i > 1000$	Polson (1950)
$k_i\left(\frac{cm}{s}\right) = 0.687 v^{\frac{1}{3}}\left(\frac{\varepsilon_b R_p}{D_{mi}}\right)^{-\frac{2}{3}}$	Wilson and Geankoplis (1966)

Table 3. Operating conditions used in experimental runs of individual proteins to determine the parameters of the different elution relationships

	Dye-ligand	Protein A
Flow (ml/min)	0.1	1
Injection volume (μl)	500	100
Protein concentration (mg/ml)	1	0.15
Gradient length (cv)	5.5	10
Modulator initial concentration (M)/initial pH	0.05	7
Modulator final concentration (M)/final pH	1	3

Table 4. Operating conditions used in experimental runs of mixtures of proteins with affinity to Protein A

Mixture	C_0 (mg/ml)			F (ml/min)	Vm (ml)	Grad (cv)
	IgG1	IgG2a	IgG2b			
(a)	0.008	0.008		1	0.5	20
(b)		0.033	0.028	1	0.1	20
(c)	0.016		0.016	1	0.5	20

Table 5. Operating conditions used in experimental runs of mixtures of proteins with affinity to cibacron blue

Mixture	C_0 (mg/ml)		F (ml/min)	Vm (ml)	Grad (cv)
	BSA	Hb			
(a)	0.75	0.75	0.10	0.5	7
(b)	0.75	0.95	0.13	0.5	5.5
(c)	0.90	0.90	0.50	0.5	10

It is important to notice that in the Blue Sepharose system, one can differentiate one elution protein peak from the other using the fact that the elution peak of Hb can be seen at 280 and 405 nm in contrast to BSA that gives maximum of absorbance just at 280 nm. This characteristic permits calculation of the concentration of each protein in the eluent fraction in a very easy way, subtracting from the absorbance profile at 280 nm the corresponding absorbance of the Hb to obtain the BSA absorbance profile (Li *et al.*, 2004).

RESULTS AND DISCUSSION

The kinetic parameters of the five proteins studied in this work (Tables 6–9) were determined using both a genetic algorithm (Carroll, 1999) and the Matlab® routine *fminsearch* minimizing the difference between experimental and simulated data given the physical parameters presented in Table 1 and the estimated values of the tested kinetic parameters. In almost all of the cases studied (except for Hb) using both the power law and exponential elution (adsorption/desorption) relationship, individual proteins were simulated with very little difference in the retention time (below 2% of relative error, Tables 10 and 11) and with very high

Table 6. Dimensionless and kinetic parameters used to simulate chromatograms of individual and mixtures of proteins with affinity to Protein A using the power law elution relationship

	τ_{tor}	N_r	Da^d	γ	a	R^2
IgG1	2	2	2.375	2.146	−8.67	0.9957
IgG2a	2	2	10.067	2.282	−8.40	0.9954
IgG2b	2	2	0.750	3.848	−13.17	0.9967

Table 7. Dimensionless and kinetic parameters used to simulate chromatograms of individual and mixtures of proteins with affinity to Protein A using the exponential type elution relationship

	τ_{tor}	N_r	Da^a	β'	a'	R^2
IgG1	4	3	12.47	−22.23	15.08	0.9977
IgG2a	4	3	29.63	−30.62	1.40	0.9963
IgG2b	4	3	28.69	−22.58	0.21	0.9946

Table 8. Dimensionless and kinetic parameters used to simulate chromatograms of individual and mixtures of proteins with affinity to cibacron blue using the power law elution relationship

	τ_{tor}	N_r	Da^d	γ	a	R^2
BSA	6	2	0.437	−13.77	8.20	0.9925
Hb	6	2	0.205	−20.01	5.98	0.9929

Table 9. Dimensionless and kinetic parameters used to simulate chromatograms of individual and mixtures of proteins with affinity to cibacron blue using the exponential type elution relationship

	τ_{tor}	N_r	Da^a	β'	a'	R^2
BSA	2	3	2.284	0.055	308.98	0.9562
Hb	2	3	0.407	0.007	679.48	0.7413

Table 10. Comparison between experimental and simulated retention times (t_{ret}) obtained from chromatograms of individual and mixtures of proteins with affinity to Protein A

	t^1_{ret}					t^2_{ret}				
	Exp	Sim_p	Error (%)	Sim_E	Error (%)	Exp	Sim_p	Error (%)	Sim_E	Error (%)
IgG1	7.91	7.91	0.0	7.91	0.0					
IgG2a	8.09	8.12	0.4	8.12	0.0					
IgG2b	8.84	8.84	0.0	8.87	0.3					
(a)	9.47	9.21	2.7	9.50	0.3					
(b)	9.61	9.28	3.4	9.61	0.0	10.93	10.27	6.0	11.22	2.7
(c)	9.21	8.88	3.6	9.06	1.6	10.93	10.38	5.0	10.67	2.4

Exp, experimental data; Sim_p, data simulated with power law elution relationship; Sim_E, data simulated with exponential type elution relationship. The Error is defined as $\left|1 - \frac{Sim}{Exp}\right|.100$.

Table 11. Comparison between experimental and simulated retention times (t_{ret}) obtained from chromatograms of individual and mixtures of proteins with affinity to cibacron blue

	t^1_{ret}					t^2_{ret}				
	Exp	Sim_p	Error (%)	Sim_E	Error (%)	Exp	Sim_p	Error (%)	Sim_E	Error (%)
BSA	59.90	59.47	0.71	60.96	1.78					
Hb	48.38	48.60	0.45	56.91	17.62					
(a)	79.05	79.40	0.40	89.22	12.90	96.26	93.14	3.20	97.07	0.80
(b)	61.18	61.08	0.20	65.61	7.20	70.32	68.63	2.40	71.65	1.90
(c)	11.25	9.88	12.20	11.84	5.30	13.76	13.81	0.30	11.84	13.90

Exp, experimental data; Sim_p, data simulated with power law elution relationship; Sim_E, data simulated with exponential type elution relationship. The Error is defined as $\left|1 - \frac{Sim}{Exp}\right|.100$.

values of a linear correlation coefficient between experimental and simulated absorbance at 280 nm (greater than 0.95 except for Hb in the exponential elution relationship with a correlation coefficient of 0.74). The reason for the differences between the experimental and simulated data of hemoglobin using the exponential relationship is the highly asymmetric shape of its elution curve that cannot be simulated using this correlation.

Mixtures of proteins with affinity to Protein A

As shown in Figures 1 and 2, the proteins with affinity to Protein A (IgG1, IgG2a, and IgG2b) elute presenting very symmetrical peaks that allow simulating elution chromatograms using both the power law and the exponential relationships. Figures 3 and 4 show experimental and simulated chromatograms of protein

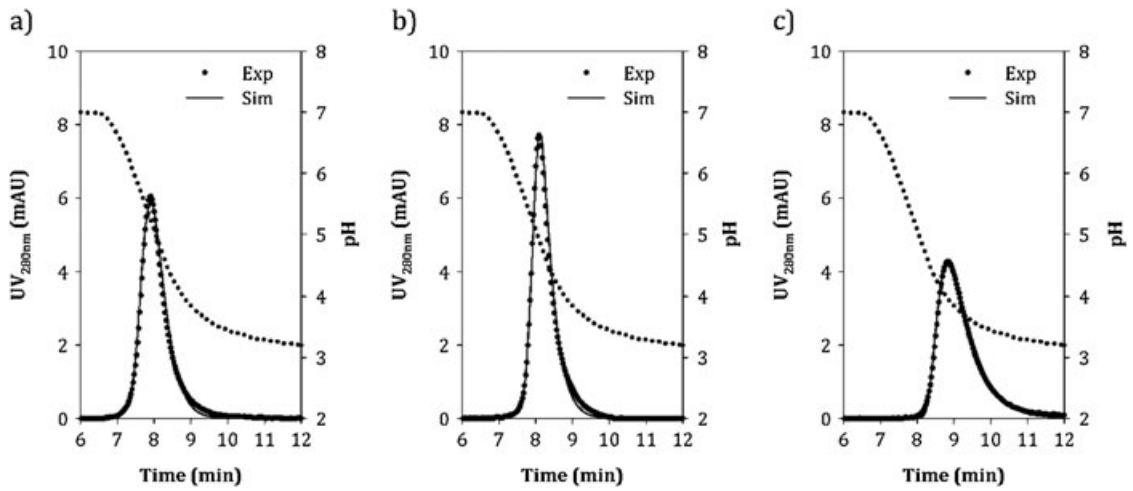

Figure 1. Individual protein elution curves fitted to experimental data (dots) using the power law elution relationship: (a) IgG1, (b) IgG2a, and (c) IgG2b. The kinetic parameters obtained are listed in Table 6, and the operating conditions used in these runs are presented in Table 3.

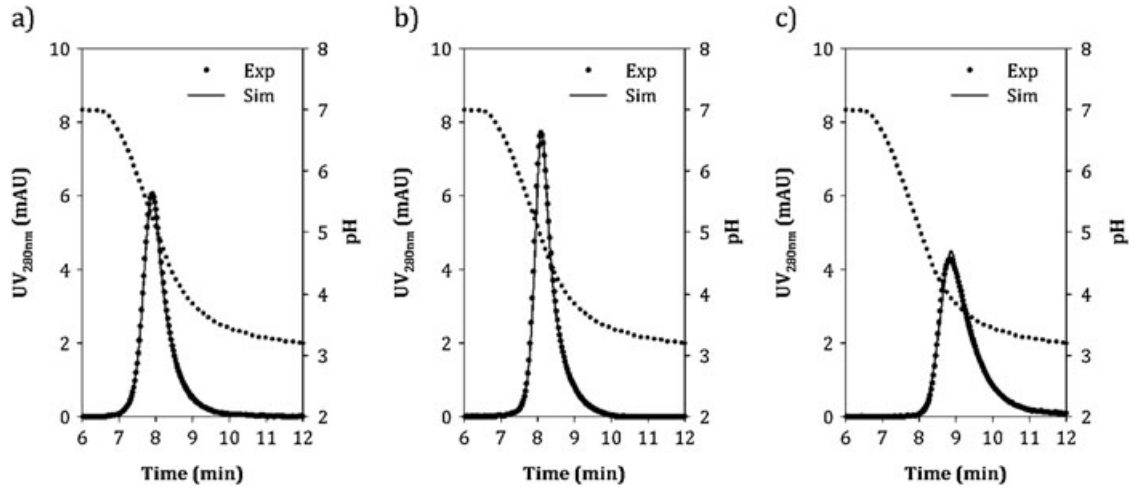

Figure 2. Individual protein elution curves fitted to experimental data (dots) using the exponential type elution relationship: (a) IgG1, (b) IgG2a, and (c) IgG2b. The kinetic parameters obtained are listed in Table 7, and the operating conditions used in these runs are presented in Table 3.

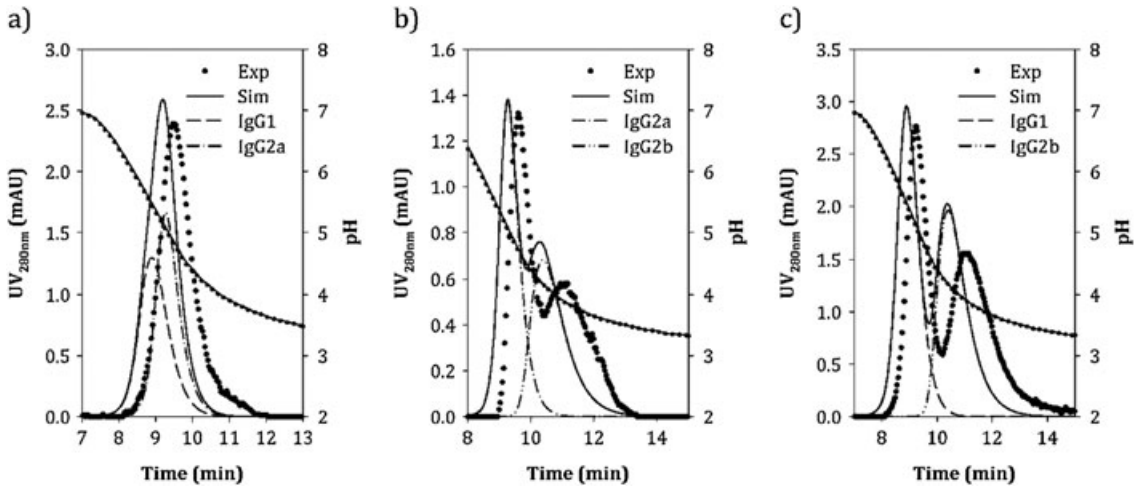

Figure 3. Comparison between experimental (dotted line) and simulated (continuous line) chromatograms of mixtures of proteins with affinity to Protein A using the power law elution relationship: (a) IgG1 + IgG2a, (b) IgG2a + IgG2b, and (c) IgG1 + IgG2b. The operating conditions used in these experiments are presented in Table 4.

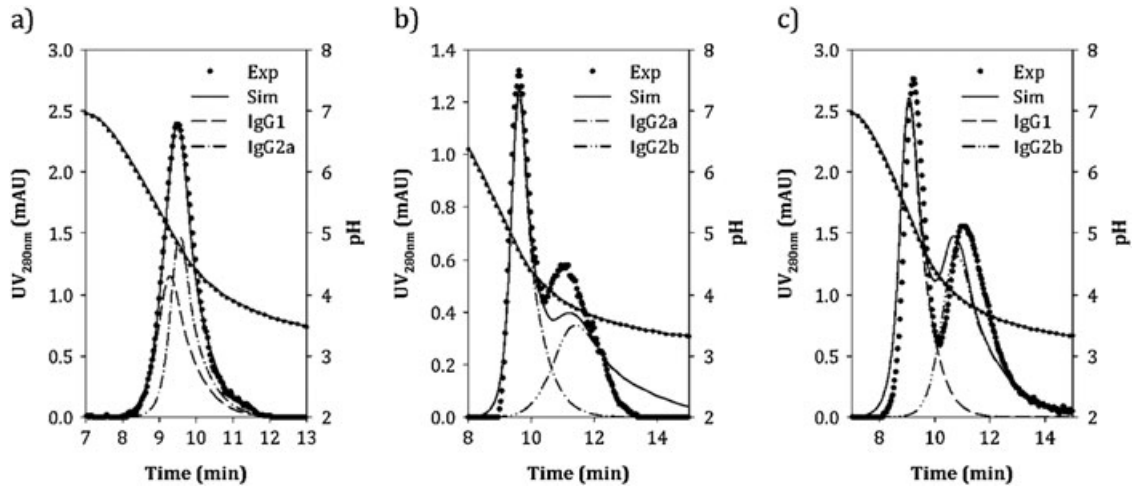

Figure 4. Comparison between experimental (dots) and simulated (continuous line) chromatograms of mixtures of proteins with affinity to Protein A using the exponential type elution relationship: (a) IgG1 + IgG2a, (b) IgG2a + IgG2b, and (c) IgG1 + IgG2b. The operating conditions used in these experiments are presented in Table 4.

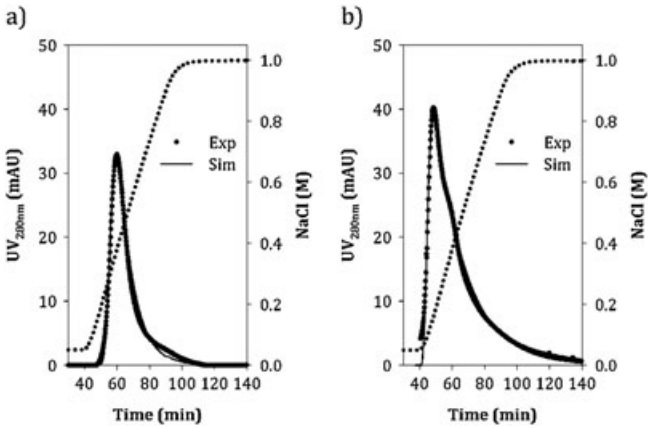

Figure 5. Individual protein elution curves fitted to experimental data (dots) using the power law elution relationship: (a) BSA and (b) Hb. The kinetic parameters obtained are listed in Table 8, and the operating conditions used in these runs are presented in Table 3.

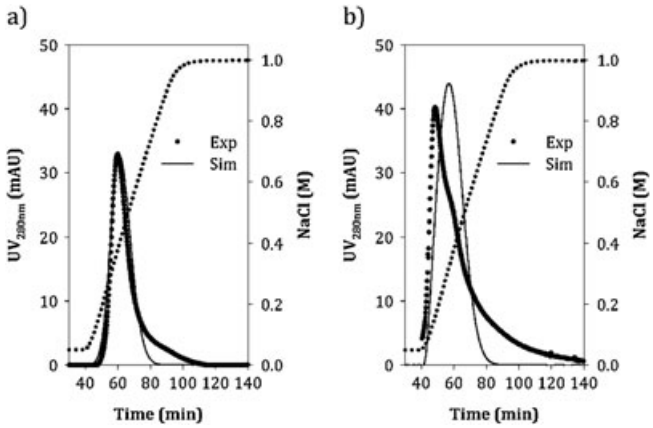

Figure 6. Individual protein elution curves fitted to experimental data (dots) using the exponential type elution relationship: (a) BSA and (b) Hb. The kinetic parameters obtained are listed in Table 9, and the operating conditions used in these runs are presented in Table 3.

mixtures. In general, these two correlations permit simulation of the elution curves with values of the linear correlation coefficient greater than 0.9 and with relative errors in the retention times smaller than 7% for variations up to 30% in the gradient length, 30% in the mobile phase flux, 400% in the injection volume, and 100% in the concentration of the proteins in the mixture as shown in Table 10. The major difference is presented for a variation of a 100% in the gradient length (Figure 3 and 4) where the power relationship is not able to properly simulate the elution curves resulting in values of the correlation coefficient below 0.7 in contrast to the values greater than 0.93 obtained with the exponential relationship. According to this, comparing both elution relationships, the best to simulate this kind of peaks (more symmetrical) should be the exponential one. In the protein mixture (Figures 3 and 4), it appears that the experimental values give longer elution times for the proteins in the column, and this behavior seems better simulated by the exponential relationship.

Mixtures of proteins with affinity to cibacron blue

The simulations fitted to the experimental data of individual proteins are shown in Figures 5 and 6 where it is evident that the power law relationship (with correlation coefficients greater than 0.99) permits a better simulation than the exponential one (with correlation coefficients equal to 0.96 for BSA and 0.74 for Hb). In the case of the protein mixtures (Figures 7 and 8), both elution relationships had problems to simulate accurately the shape of the BSA curve, probably because of heterogeneity of commercial BSA samples (the BSA elutes with different peaks that can be seen using smoother gradients). This behavior has been reported before (Hunter and Carta, 2001; Susanto *et al*., 2006; Sandoval *et al*., 2010). From Table 11, it can be seen that although the exponential relationship shows relative errors in the retention times of the peaks in the mixtures up to 15% for variations up to 30% in the mobile phase flux and up to 82% in the gradient length, one can more or less predict the fractions where the Hb and the BSA in the mixture are going to elute as can be seen in Figure 9 (a) II and (b) II. Figure 9 shows the experimental values of individual peaks of BSA and Hb because, as stated in the Materials and Methods section, these can be calculated from ultraviolet

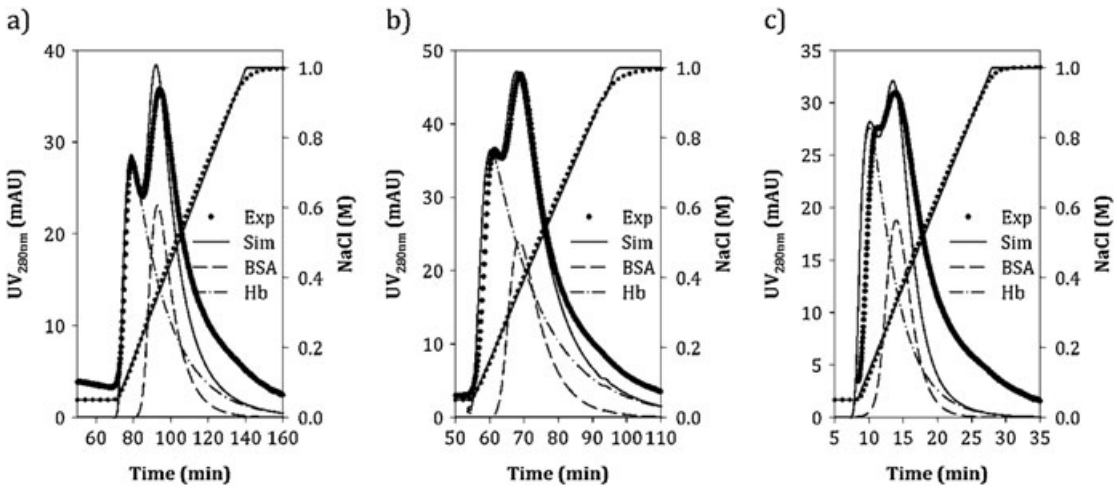

Figure 7. Comparison between experimental (dotted line) and simulated (continuous line) chromatograms of mixtures of proteins with affinity to cibacron blue using the power law elution relationship: (a) 0.75 mg/ml BSA, 0.75 mg/ml Hb; (b) 0.75 mg/ml BSA, 0.95 mg/ml Hb; and (c) 0.90 mg/ml BSA, 0.90 mg/ml Hb. The operating conditions used in these experiments are presented in Table 5.

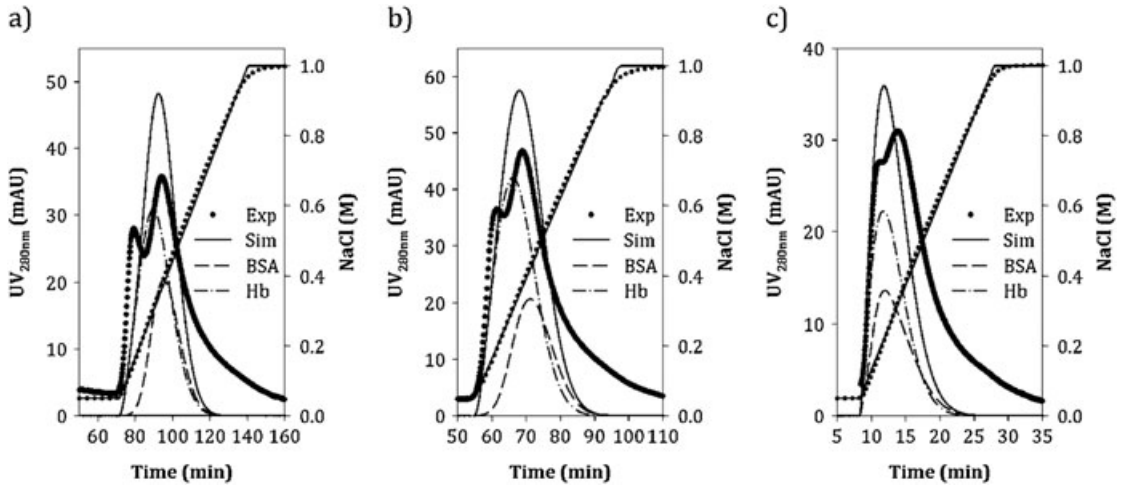

Figure 8. Comparison between experimental (dotted line) and simulated (continuous line) chromatograms of mixtures of proteins with affinity to cibacron blue using the exponential type elution relationship: (a) 0.75 mg/ml BSA, 0.75 mg/ml Hb; (b) 0.75 mg/ml BSA, 0.95 mg/ml Hb; and (c) 0.90 mg/ml BSA, 0.90 mg/ml Hb. The operating conditions used in these experiments are presented in Table 5.

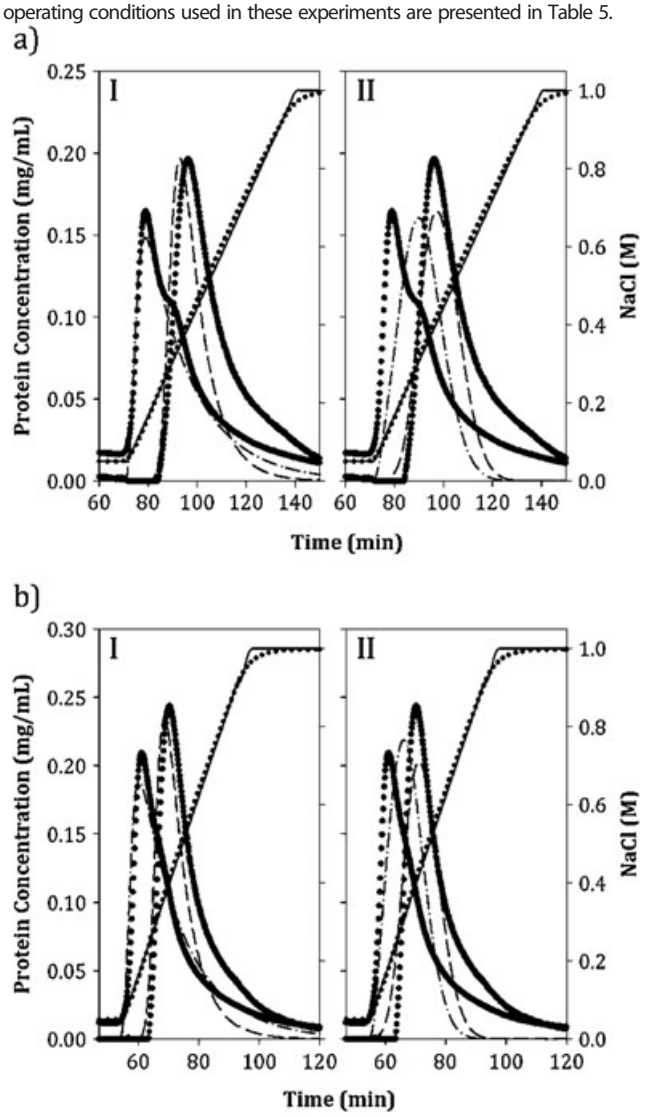

Figure 9. Comparison between experimental and simulated data of (a) mixtures and (b) proteins with affinity to cibacron blue using (I) power law elution relationship and (II) exponential type elution relationship. The experimental data corresponds to the dotted lines and the peaks correspond to BSA (first elution peak) and Hb (second elution peak).

measurements at two wavelengths. Nevertheless, the power law relationship always shows better results with relative errors lower than 10% for the same variations in the gradient length and for variations up to 400% in the mobile phase flux and, moreover, permits observation of both of the peaks in a curve of absorbance at 280 nm versus time (Figure 7) in contrast with the curves calculated using the exponential relationship (Figure 8), making this eluate–modulator relationship the desired one in cases where asymmetrical peaks are obtained during elution chromatography.

CONCLUSIONS

Affinity elution chromatography was modeled, and two different systems (Blue Sepharose and Protein A) were simulated using a general rate model and two different eluate–modulator relationships: a power law relationship and an exponential type elution (adsorption/desorption) relationship. With Blue Sepharose, a linear salt gradient was used, and with Protein A, a semi-linear pH gradient. In both cases, kinetic parameters involved in the different elution correlations for each of the five individual proteins studied were determined using a genetic algorithm and the Matlab® routine *fminsearch* resulting in very good fittings of the experimental data (with linear correlation coefficients greater than 0.99 in most of the cases). The exponential relationship permits simulation of the elution curves of proteins with affinity to Protein A with relative errors in the retention times below 3% for variations up to 30% in the mobile phase flux and up to 100% in the gradient length. Clearly, these peaks are more symmetrical, and the exponential relationship gives a slightly better fit of these types of peak. For the proteins with affinity to cibacron blue, the power law relationship showed better results than the exponential one, with relative errors in the retention times below 7% for variations up to 30% in the mobile phase flux and up to 82% in the length of the gradient. These peaks are clearly much more asymmetrical. In general, the exponential relationship studied permits simulation of more symmetrical peaks giving better results than the power relationship for bigger variations in the gradient length. In contrast, the power relationship permits more accurate simulation of the shape of more asymmetrical peaks like the one presented by the hemoglobin studied in this work.

NOMENCLATURE

a_i Constant in Langmuir isotherm for component i, $C^{\infty}b_i$

b_i Adsorption equilibrium constant for component i, $\frac{k_{ai}}{k_{di}}$

Bi_i Biot number for mass transfer for component i, $\frac{k_i R_p}{\varepsilon_p D_{pi}}$

BSA Bovine serum albumin

C_{oi} Maximum concentration of protein i, equal to initial feed concentration of the component $\max_{(i c_{fi}(\tau))}$

C^{∞} Maximum capacity of the column

$C_{A,N+1}$ Initial dimensionless concentration (or pH) of the modulator in the mobile phase

c_{bi} Dimensionless concentration of component i in the bulk fluid phase

$C_{fi}(\tau)$ Feed concentration of component i

$\bar{c_{pi}}$ Dimensionless concentration of component i adsorbed to the resin

$c_{pi,r=1}$ Dimensionless concentration of component i in the exterior of the porous particle

d Inner diameter of the column

d_{porous} Macroporous particle diameter

Da_i^a Damkhöler number for adsorption of component i, $\frac{Lk_{ai}C_{oi}}{v}$

Da_i^d Damkhöler number for desorption of component i, $\frac{Lk_{di}}{v}$

D_{bi} Axial dispersion coefficient of component i

d_{mi} Solute molecule diameter

D_{mi} Molecular diffusivity

D_{pi} Effective diffusivity of component i

Error Relative error (in %) between experimental and simulated data, $\left|1-\frac{\mathrm{Sim}}{\mathrm{Exp}}\right|.100$

Exp Experimental data

F Flux of the mobile phase

Grad Gradient length

Hb Rabbit hemoglobin

k_{ai} Adsorption rate constant for component i

k_{di} Desorption rate constant for component i

k_i Mass transfer coefficient of component i

L Column length

MW_i Molecular weight of protein i

N Number of proteins present in the sample. The modulator corresponds to the component $N+1$

N_e Number of quadratic elements in the finite element discretization method

N_r Number of interior collocation points in the orthogonal collocation discretization method

Pe_{Li} Peclet number for mass transfer for component i, $\frac{vL}{D_{bi}}$

r Dimensionless radial coordinate

Re Reynolds number, $\frac{2\rho_l v R_p}{\mu_l}$

R_p Radius of the adsorbent particle

Sim Simulated data

v Interstitial velocity, $\frac{4F}{\tau d^2 \varepsilon_b}$

Vm Sample volume

z Dimensionless axial coordinate

Greek letters

a_i, γ_i Experimental parameters for the powered elution relationshipa_i', β_i' Experimental parameters for the exponential elution relationship

ε_b Bed void volume fraction

ε_{pi} Adsorbent particle porosity for component i

η_i Dimensionless parameter for component i, $\frac{\varepsilon_{pi}D_{pi}L}{R_p^2 v}$

λ_i Ratio between the solute molecule diameter and the macroporous particle diameter, $\frac{d_{mi}}{d_{\mathrm{porous}}}$

μ_l Viscosity of the mobile phase

ξ_i Dimensionless parameter for component i, $\frac{3\mathrm{Bi}_i\eta_i(1-\varepsilon_b)}{\varepsilon_b}$

ρ_l Density of the mobile phase

τ_{tor} Adsorbent particle tortuosity

τ Dimensionless time

Acknowledgements

The authors acknowledge the Millennium Scientific Initiative for financial support (ICM-P05-001-F) and Conicyt for a doctoral scholarship (G.S.).

REFERENCES

Carroll DL. 1999. D. L. Carroll's FORTRAN Genetic Algorithm Driver, http://cuaerospace.com/carroll/ga.html [March 2009].

Chung SF, Wen CY. 1968. Longitudinal dispersion of liquid flowing through fixed and fluidized beds. *AIChE J* **14**: 857-866.

Gallant SR, Vunnum S, Cramer SM. 1996. Modeling gradient elution of proteins in ion-exchange chromatography. *AIChE J* **42**: 2511–2520.

Geankoplis CJ. 1998. Transport processes and unit operations. 3rd edition. Prentice Hall International: Mexico.

Gu T. 1995. Mathematical modeling and scale-up of liquid chromatography. Springer: Berlin, New York.

Gu T, Zheng Y. 1999. A study of the scale-up of reversed-phase liquid chromatography. *Sep Pur Technol* **15**: 41–58.

Gu T, Truei YH, Tsai GJ, Tsao GT. 1992. Modeling of gradient elution in multicomponent nonlinear chromatography. *Chem Eng Sci* **47**: 253–262.

Gu T, Hsu KH, Syu MJ. 2003. Scale-up of affinity chromatography for purification of enzymes and other proteins. *Enzyme Microb. Technol.*, **33**: 430–437.

Hage DS, Bian M, Burks R, Karle E, Ohnmacht C, Wa C. 2006. Bioaffinity-Chromatography. Chapter 5 of Handbook of Affinity Chromatography, Hage DS (ed) Second edition. Lund, Sweden. Taylor & Francis Group.

Hunter AK, Carta G. 2001. Effects of bovine serum albumin heterogeneity on frontal analysis with anion-exchange media. *J. Chromatogr. A* **937**: 13–9.

Li Z, Gu Y, Gu T. 1998. Mathematical modeling and scale-up of size-exclusion chromatography. *Biochem. Eng. J.* **2**: 145–155.

Li W, Zhang S, Sun Y. 2004. Modeling of the linear-gradient dye-ligand affinity chromatography with a binary adsorption isotherm. *Biochem. Eng. J.* **22**: 63–70.

Lienqueo ME, Shene C, Asenjo JA. 2009. Optimization of hydrophobic interaction chromatography using a mathematical model of elution curves of a protein mixture. *J. Mol. Recognit.* **22**: 110–20.

Melander WR, El Rassi Z, Horvath C. 1989. Interplay of hydrophobic and electrostatic interactions in biopolymer chromatography. Effect of salts on the retention of proteins. *J. Chromatogr.* **469**: 3–27.

Orellana CA, Shene C, Asenjo JA. 2009. Mathematical modeling of elution curves for a protein mixture in ion exchange chromatography applied to high protein concentration. *Biotechnol. Bioeng.* **104**: 572–81.

Polson A. 1950. Some aspects of diffusion in solution and a definition of a colloidal particle. *J. Phys Colloid. Chem.* **54**: 649-652.

Sandoval G, Shene C, Andrews B A, Asenjo JA. 2010. Extension of the selection of protein chromatography and the rate model to affinity chromatography. *J. Mol. Recognit.* **23**: 609–17.

Shene C, Lucero A, Andrews B A, Asenjo, JA. 2006. Mathematical modeling of elution curves for a protein mixture in ion exchange chromatography and for the optimal selection of operational conditions. *Biotechnol. Bioeng.* **95**: 704–13.

Susanto A, Wekenborg K, Hubbuch J, Schmidt-Traub H. 2006. Developing a chromatographic column model for bovine serum albumin on strong anion-exchanger Source30Q using data from confocal laser scanning microscopy. *J. Chromatogr. A* **1137**: 63–75.

Wilson EJ, Geankoplis CJ. 1966. Liquid mass transfer at very low Reynolds numbers in packed beds. *In dEng Chem Fundam* **5**: 9–17.

Yamamoto S, Nakanishi K, Matsuno R, Kamikubo T. 1983. Ion exchange chromatography of proteins-prediction of elution curves and operating conditions. I. Theoretical considerations. *Biotechnol. Bioeng.*, **25**: 1465–83.

Yau WW, Kirkland JJ, Bly DD. 1979. Modern size exclusion liquid chromatography. Wiley: New York.